JOURNAL OF GUIDANCE, CONTROL, AND DYNAMICS
Vol. 20, No. 5, September–October 1997

Trajectory Matching Flight-Path Optimization of Aerospace Vehicles

Rush D. Robinett* and G. Richard Eisler†
Sandia National Laboratories, Albuquerque, New Mexico 87185

A new class of six-degree-of-freedom optimization problems referred to as trajectory matching flight-path optimization is addressed and explicitly described via an example problem. The essence of this class of flight-path optimization problems is to force an aerospace vehicle to follow prescribed translational and rotational velocity histories or to motion-match. For this example, a lightweight, axisymmetric re-entry vehicle decoy is designed to match the motion of a typical full-weight re-entry vehicle by optimizing its mass properties. The optimization problem, which is performed in two steps, is given as the minimization of the difference between the target trajectory and the actual trajectory subject to physical constraints. The first step utilizes a unique stability measure to develop similarity parameters that provide excellent initial guesses for the numerical optimization routine employed in the second step. The second step utilizes a sequential quadratic programming algorithm to numerically solve the constrained minimization problem. Simulation results demonstrate the robust trajectory matching of the lightweight re-entry vehicle.

I. Introduction

THE preliminary design of an aerospace vehicle entails choosing a basic planform from among many different conceptual ideas. The basic planform must enable the vehicle to perform a prescribed mission within an acceptable flight envelope while satisfying certain physical constraints. In most cases, the physical constraints define feasible regions from which to choose but do not provide exact values of the planform dimensions. As a result, the preliminary designer must determine the planform dimensions, one hopes in some optimum fashion, to satisfy the mission requirements.

Typically, the basic planform dimensions are established using a point mass analysis in a variety of numerical ways.[1–4] The point mass analysis is often referred to as trajectory optimization because good translational information usually can be obtained without rigorously including the dynamics associated with the rotational degrees of freedom (DOF). In particular, the body orientation is artificially constrained, for example, to maintain zero angle of attack. Although useful translational trajectory information is acquired, point mass analyses do not deliver detailed rotational motions or include the effects of dynamic coupling. Consequently, if one is interested in six-DOF optimization, the point mass trajectories usually represent a starting point for further investigation.

This paper contributes to the methodology for six-DOF optimization by addressing a new class of problems. The new class of problems is referred to as trajectory matching flight-path optimization. The essence of this flight-path optimization procedure is to force a vehicle to follow (as nearly as possible) prescribed translational and rotational velocity histories or to motion-match. The target trajectory is assumed to be specified in advance, and the general form of the optimization problem is given as the minimization of the difference between the target trajectory and the actual trajectory subject to physical constraints. The minimization process is performed in two steps. The first step utilizes a unique stability measure, referred to as stability of motion matching (SMM),[5,6] to develop similarity parameters that provide excellent initial guesses for the numerical optimization routine employed in the second step. The second step utilizes a sequential quadratic programming (SQP) algorithm[7] to numerically solve the constrained minimization problem. The performance index is a time integral of the weighted squared residuals of the flight-path errors, and the optimization parameters are the mass properties of the vehicle.

To explicate the design process, a lightweight (10% of the mass), axisymmetric re-entry vehicle (RV) decoy was designed to match the six-DOF motion, i.e., translational and rotational velocity histories, of a typical full-weight RV. To match the six-DOF motion of a full-weight RV, the mass properties of the lightweight RV, which has an identical external geometry, i.e., the same aerodynamic properties, were judiciously chosen. The initial assumption in the design process is that the dynamics of both RVs can be forced to be identical. The dynamics can never be identical in practice, but by analytically imposing this ideality via the SMM formulation, a set of similarity parameters was identified. These similarity parameters were used to initialize the SQP algorithm and to develop a lightweight dynamical match of the full-weight RV.

The rest of the paper is divided into five sections. Section II derives the equations of motion for an axisymmetric RV, and Sec. III develops the concept of SMM. Section IV defines the optimization problem, and Secs. V and VI provide the results and conclusions.

II. Equations of Motion

The equations of motion for an axisymmetric RV are derived from Newton's laws in vector form. The RV is assumed to have constant mass with its center of mass location defined relative to a fixed reference point o inside the body (Fig. 1). The principal moments of inertia are assumed to be collinear with the geometric axes of symmetry, and the external forces and torques are due to gravity and aerodynamic loading. The equations of motion relative to the nonrolling frame are[6,8]

$$\boldsymbol{F} = m[\dot{\boldsymbol{V}} + \boldsymbol{\omega}_{\mathrm{N/I}} \times \boldsymbol{V} + \dot{\boldsymbol{\omega}}_{\mathrm{N/I}} \times \boldsymbol{\rho}_{\mathrm{cm}} + \boldsymbol{\omega}_{\mathrm{N/I}} \times (\boldsymbol{\omega}_{\mathrm{N/I}} \times \boldsymbol{\rho}_{\mathrm{cm}})] \quad (1)$$

$$\boldsymbol{M}_o = \dot{\boldsymbol{H}} + \boldsymbol{\omega}_{\mathrm{N/I}} \times \boldsymbol{H} + m\boldsymbol{\rho}_{\mathrm{cm}} \times [\dot{\boldsymbol{V}} + \boldsymbol{\omega}_{\mathrm{N/I}} \times \boldsymbol{V}] \quad (2)$$

where

$\boldsymbol{F}$ = external forces
$\boldsymbol{H}$ = angular momentum about point o
$\boldsymbol{M}_o$ = external moments about point o
m = RV mass
$\boldsymbol{V}$ = velocity of point o
$\boldsymbol{\rho}_{\mathrm{cm}}$ = center of mass location relative to point o that is fixed in the nonrolling frame
$\boldsymbol{\omega}_{\mathrm{N/I}}$ = rotation rate of the nonrolling frame relative to the inertial frame

Received Feb. 26, 1996; revision received April 14, 1997; accepted for publication April 26, 1997.

*Distinguished Member, Technical Staff, P.O. Box 5800. Associate Fellow AIAA.
†Senior Member, Technical Staff, P.O. Box 5800. Associate Fellow AIAA.

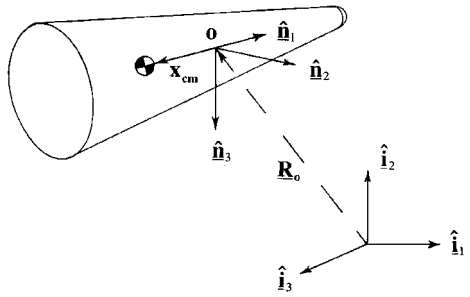

Fig. 1 Coordinate systems.

A nonrolling frame is used to analyze the motion of the RVs because both vehicles are axisymmetric (no useful roll information), and these equations are numerically more stable than the equivalent body-fixed equations of motion. As a result, the typical 3-2-1 rotation sequence (yaw, pitch, roll) can be reduced to only a 3-2 sequence:

$$\{\hat{\boldsymbol{i}}\} = [C(\psi, \theta)]\{\hat{\boldsymbol{n}}\} \tag{3}$$

where

$\{\hat{\boldsymbol{i}}\}$ = unit vector defining the inertial frame
$\{\hat{\boldsymbol{n}}\}$ = unit vector defining the nonrolling frame
θ = pitch Euler angle
ψ = yaw Euler angle

and

$$[C(\psi, \theta)] = \begin{bmatrix} \cos\theta\cos\psi & -\sin\psi & \sin\theta\cos\psi \\ \cos\theta\sin\psi & \cos\psi & \sin\theta\sin\psi \\ -\sin\theta & 0 & \cos\theta \end{bmatrix} \tag{4}$$

The state-space equations that result from the combination of Eqs. (1–3) are given next. The state vector is defined as

$$\boldsymbol{x} = (X_o, Y_o, Z_o, \psi, \theta, u, v, w, \bar{p}, q, r)^T \tag{5}$$

where

$$\boldsymbol{V} = u\hat{\boldsymbol{n}}_1 + v\hat{\boldsymbol{n}}_2 + w\hat{\boldsymbol{n}}_3 = \dot{X}_o\hat{\boldsymbol{i}}_1 + \dot{Y}_o\hat{\boldsymbol{i}}_2 + \dot{Z}_o\hat{\boldsymbol{i}}_3$$

$$\boldsymbol{\omega}_{\mathrm{N/I}} = p\hat{\boldsymbol{n}}_1 + q\hat{\boldsymbol{n}}_2 + r\hat{\boldsymbol{n}}_3$$

and $\bar{p}$ is the body-fixed roll rate.

The translational velocity of point o in the inertial frame is

$$\begin{pmatrix} \dot{X}_o \\ \dot{Y}_o \\ \dot{Z}_o \end{pmatrix} = [C(\psi, \theta)] \begin{pmatrix} u \\ v \\ w \end{pmatrix}$$

and the Euler angle rates are

$$\begin{pmatrix} \dot{\psi} \\ \dot{\theta} \end{pmatrix} = \begin{pmatrix} r/\cos\theta \\ q \end{pmatrix}$$

The translational accelerations in the nonrolling frame are

$$\begin{pmatrix} \dot{u} \\ \dot{v} \\ \dot{w} \end{pmatrix} = \begin{Bmatrix} \left(F_{A_x}/m\right) + g_x - qw + rv + x_{\mathrm{cm}}(q^2 + r^2) \\ \left(F_{A_y}/m\right) + g_y - ru + pw - x_{\mathrm{cm}}\left[I - mx_{\mathrm{cm}}^2\right]^{-1}\left(M_{A_z} - x_{\mathrm{cm}}F_{A_y} + I_{xx}\bar{p}q\right) \\ \left(F_{A_z}/m\right) + g_z - pv + qu + x_{\mathrm{cm}}\left[I - mx_{\mathrm{cm}}^2\right]^{-1}\left(M_{A_y} + x_{\mathrm{cm}}F_{A_z} - I_{xx}\bar{p}r\right) \end{Bmatrix} \tag{6}$$

and the body-fixed roll and nonrolling pitch and yaw accelerations are

$$\begin{pmatrix} \dot{\bar{p}} \\ \dot{q} \\ \dot{r} \end{pmatrix} = \begin{Bmatrix} M_{A_x}/I_{xx} \\ \left[I - mx_{\mathrm{cm}}^2\right]^{-1}\left(M_{A_y} + x_{\mathrm{cm}}F_{A_z} - I_{xx}\bar{p}r\right) + pr \\ \left[I - mx_{\mathrm{cm}}^2\right]^{-1}\left(M_{A_z} - x_{\mathrm{cm}}F_{A_y} + I_{xx}\bar{p}q\right) - pq \end{Bmatrix} \tag{7}$$

where

$F_{A_x}, F_{A_y}, F_{A_z}$ = aerodynamic forces
g_x, g_y, g_z = gravity components
I_{xx}, I = roll and pitch (yaw) moments of inertia
$M_{A_x}, M_{A_y}, M_{A_z}$ = aerodynamic moments
p = nonrolling roll rate, $-\dot{\psi}\sin\theta$

III. SMM

The SMM concept begins with the stability of a motion as described by Willems.[9] The stability of a motion is used to assess the stability of a system trajectory that over time may not converge to a single equilibrium point in the phase hyperplane. A motion $\boldsymbol{x}(t; \boldsymbol{x}_0, t_0)$ is stable if, for any t_0 and $\varepsilon > 0$, there exists a $\delta(\varepsilon, t_0) > 0$ such that

$$\|\boldsymbol{x}(t; \boldsymbol{x}_0, t_0) - \boldsymbol{x}(t; \boldsymbol{x}_1, t_0)\| < \varepsilon \tag{8}$$

for

$$\|\boldsymbol{x}_0 - \boldsymbol{x}_1\| < \delta \qquad \text{and all} \qquad t \geq t_0$$

Figure 2 presents a pictoral interpretation of the preceding definition.

The stability of a motion is modified to develop the SMM formulation.[5,6] A vehicle that is described by $\boldsymbol{f}_1$ is ε-stable with respect to motion-matching if, for any t_0, any $\boldsymbol{x}_0$, and an $\varepsilon > 0$,

$$\|\boldsymbol{x}(t; \boldsymbol{x}_0, t_0) - \tilde{\boldsymbol{x}}(t; \boldsymbol{x}_0, t_0)\|_K < \varepsilon \tag{9}$$

with

$$\dot{\boldsymbol{x}} = \boldsymbol{f}_1(\boldsymbol{x}, t) \qquad \text{and} \qquad \dot{\tilde{\boldsymbol{x}}} = \boldsymbol{f}_2(\tilde{\boldsymbol{x}}, t)$$

and for all $t \geq t_0$, where $\boldsymbol{f}_2$ defines the reference (target) vehicle dynamics. The specific form of the weighted norm in Eq. (9) is

$$\begin{aligned} &\|\boldsymbol{x}(t; \boldsymbol{x}_0, t_0) - \tilde{\boldsymbol{x}}(t; \boldsymbol{x}_0, t_0)\|_K \\ &\quad = \left\|\boldsymbol{k}^T \cdot [\boldsymbol{x}(t; \boldsymbol{x}_0, t_0) - \tilde{\boldsymbol{x}}(t; \boldsymbol{x}_0, t_0)]\right\|_\infty \\ &\quad = \max_i |k_i[x_i(t; \boldsymbol{x}_0, t_0) - \tilde{x}_i(t; \boldsymbol{x}_0, t_0)]| \end{aligned}$$

where k_i is the ith normalization constant. The modifications to the original definition take on the forms of two separate sets of state equations (system models), a weighted norm, and the application of uniform boundedness [refer to the first of Eqs. (9)]. The two sets of equations replace the original single-set formulation because the motion-matching criteria force one vehicle to follow the motion of a reference or target vehicle given the same initial conditions.

The weighted norm is utilized to provide a deviation measure between the two vehicles that can be interpreted as a percentage measure. In fact, if the weights are chosen properly, i.e., the ith weight is chosen as the inverse of the maximum value of the ith state along the trajectory of interest, the weighted deviation of Eq. (9) is approximately the percentage error of the deviation of the actual trajectory from the target trajectory. As a result, the value of ε is simply chosen as the amount of percentage error that can be tolerated by the mission requirements.

The definition of uniform boundedness is used to describe the deviation of one vehicle from the other. The deviation is required to be bounded by a prescribed ε that is not a function of either the initial time or the initial state. In other words, the deviation must be bounded by a single perturbation limit no matter what initial times or states are chosen.

To illustrate the SMM formulation, the similarity parameters for the design of an axisymmetric RV are derived by setting $\varepsilon = 0$,

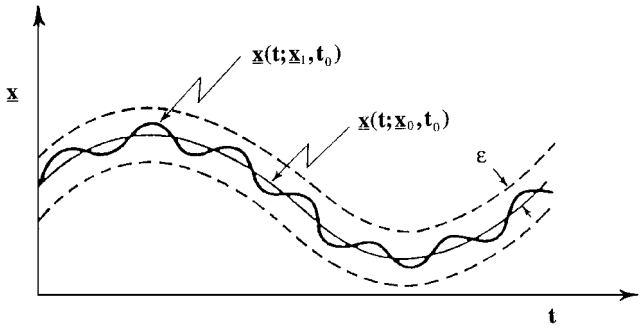

Fig. 2 Stability of a motion.

which implies perfect motion-matching. Perfect motion-matching occurs when the accelerations and velocities of each RV are identical given the same initial conditions. This situation implies that

$$\dot{\boldsymbol{x}} - \dot{\tilde{\boldsymbol{x}}} = \mathbf{0} \tag{10}$$

and

$$\boldsymbol{x} - \tilde{\boldsymbol{x}} = \mathbf{0} \tag{11}$$

Although perfect motion-matching cannot be obtained, the resulting similarity parameters provide excellent initial guesses for the numerical optimization process and provide design rules of thumb. Because both vehicles are initialized with the same state vector, the velocity variables are the only trajectory time histories of interest. The position variables are removed from the SMM formulation by zeroing the appropriate weights. The optimization parameters that are incorporated into the similarity parameters are the mass properties (m, x_{cm}, I_{xx}, I) of the lightweight RV, which are subscripted 1, and the full-weight RV parameters are subscripted 2. By applying Eqs. (9–11) to the dynamics of the lightweight RV ($\boldsymbol{x}$) and the full-weight RV ($\tilde{\boldsymbol{x}}$), the similarity parameters for perfect motion-matching are given as

$$x_{\text{cm}_1} = x_{\text{cm}_2} \tag{12}$$

$$\frac{I_{xx_1}}{I_1 - m_1 x_{\text{cm}_1}^2} = \frac{I_{xx_2}}{I_2 - m_2 x_{\text{cm}_2}^2} \tag{13}$$

$$F_{A_{x_1}} \big/ m_1 = F_{A_{x_2}} \big/ m_2 \tag{14}$$

$$F_{A_{y_1}} \big/ m_1 = F_{A_{y_2}} \big/ m_2 \tag{15}$$

$$F_{A_{z_1}} \big/ m_1 = F_{A_{z_2}} \big/ m_2 \tag{16}$$

$$M_{A_{x_1}} \big/ I_{xx_1} = M_{A_{x_2}} \big/ I_{xx_2} \tag{17}$$

$$\frac{M_{A_{y_1}} + x_{\text{cm}_1} F_{A_{z_1}}}{I_1 - m_1 x_{\text{cm}_1}^2} = \frac{M_{A_{y_2}} + x_{\text{cm}_2} F_{A_{z_2}}}{I_2 - m_2 x_{\text{cm}_2}^2} \tag{18}$$

$$\frac{M_{A_{z_1}} - x_{\text{cm}_1} F_{A_{y_1}}}{I_1 - m_1 x_{\text{cm}_1}^2} = \frac{M_{A_{z_2}} - x_{\text{cm}_2} F_{A_{y_2}}}{I_2 - m_2 x_{\text{cm}_2}^2} \tag{19}$$

As an example of how these similarity parameters are derived, the nonrolling axial velocity of Eqs. (6) is used to obtain Eqs. (12) and (14). First, the axial accelerations of the RVs are set equal to one another [Eq. (10)]:

$$\left(F_{A_{x_1}} \big/ m_1\right) + g_{x_1} - q_1 w_1 + r_1 v_1 + x_{\text{cm}_1}\left(q_1^2 + r_1^2\right)$$
$$= \left(F_{A_{x_2}} \big/ m_2\right) + g_{x_2} - q_2 w_2 + r_2 v_2 + x_{\text{cm}_2}\left(q_2^2 + r_2^2\right)$$

Next, Eq. (11) is used to eliminate equivalent terms (because all of the states are identical), which results in the following reduced equation:

$$\left(F_{A_{x_1}} \big/ m_1\right) + x_{\text{cm}_1}\left(q_1^2 + r_1^2\right) = \left(F_{A_{x_2}} \big/ m_2\right) + x_{\text{cm}_2}\left(q_2^2 + r_2^2\right)$$

The last step is to equate like terms, which directly results in Eqs. (12) and (14). The other similarity parameters are acquired by applying the same methodology to the body-fixed roll rate [Eq. (17)], the nonrolling pitch rate [Eqs. (13) and (18)], the nonrolling yaw rate [Eq. (19)], the nonrolling y-direction velocity [Eq. (15)], and the nonrolling z-direction velocity [Eq. (16)].

A prudent step at this point is to understand the impact of each of these similarity parameters on the design of a lightweight RV. Equations (14–16) are equivalent to matching the aeroballistic coefficients of the RVs:

$$m_1 g \big/ C_{A_x} A = m_2 g \big/ C_{A_x} A$$

where

A = reference area
C_{A_x} = aerodynamic axial force coefficient

Obviously, these similarity parameters cannot be affected by the optimization of the mass properties because only the total mass parameter is included, and these relationships would require that the masses of both RVs be identical (because the aerodynamic characteristics are the same). The effective solution to this problem is to compensate with a thrust augmentation system as described in Ref. 6, where direct control over these similarity parameters is obtained in the following manner:

$$\frac{F_{A_{x_1}} + T}{m_1} = \frac{F_{A_{x_2}}}{m_2}$$

where T is the optimal thrust history necessary to match the translational velocities by decreasing the aerodynamic deceleration. The details of obtaining the optimal thrust history and how the mass properties vary with time are not discussed because the goal of this study is to optimize the fixed (constant) mass properties of the lightweight RV.

The effects described by Eq. (17) are minimal for this design because the aerodynamic induced roll torques are small over the altitude range of interest. As a result, this constraint is neglected in the following optimization process.

Equations (12), (13), (18), and (19) are the similarity relationships of importance to this design. Even though Eq. (12) is rigorously correct, the design can violate this relationship and perform quite satisfactorily. The reason for this behavior is that Eqs. (6) are the only places where this constraint is effective, and these terms constitute a small percentage of the total translational accelerations as compared with aerodynamic forces. Consequently, this constraint is neglected during the optimization process.

Equation (13) requires that the moment of inertia ratio of the full-weight RV be maintained in the lightweight RV. This requirement is more intuitive if the torque-free coning motion of an axisymmetric RV is considered. Equation (13) can be easily derived from the torque-free equations of motion of an RV by imposing the constraint of matched coning motions.[6] Specifically, θ_C is the coning angle for torque-free motion of an axisymmetric body and is described mathematically as

$$\tan\theta_C = \frac{\left(I - m x_{\text{cm}}^2\right)\sqrt{q^2 + r^2}}{I_{xx}\bar{p}}$$

By imposing matched coning angles, $\theta_{C_1} = \theta_{C_2}$, and assuming perfect motion-matching ($q_1 = q_2$, $r_1 = r_2$, and $\bar{p}_1 = \bar{p}_2$), Eq. (13) is the direct result.

The combination of Eqs. (18) and (19) leads to the design constraints of minimizing the static margin and maximizing the pitch moment of inertia of the lightweight RV. The static margin is defined as the difference between the center of pressure and the center of mass locations relative to point o (and the nose of the RV; see Fig. 3). The static margin is a function of altitude and is calculated from the following relationship:

$$SM = \frac{x_{\text{cm}} - x_{\text{cp}}}{l_d} = \frac{x_{\text{cm}} - \left(M_{A_y} \big/ F_{A_z}\right)}{l_d}$$

where l_d is the total length of the RV. Typically, the center of pressure location moves (forward) toward the nose as the altitude decreases, which, in turn, decreases the static margin. The minimum allowable static margin is defined by the static stability requirements of the

RV. In particular, the onset of static instability is typically dictated by the altitude at which the static margin becomes negative, i.e., the center of pressure moves in front of the center of mass relative to the nose of the RV. The minimum altitude of interest usually determines the point of neutral stability (the static margin equals zero), which, in turn, dictates the most negative location of the center of mass of the RV relative to the reference point o, i.e., the RV is statically stable over the altitude range of interest. As a result, the static margin should be reduced to the length necessary to reduce the aerodynamic induced rotational accelerations on the lightweight RV to the levels on the full-weight RV, i.e., satisfy Eqs. (18) and (19), without destabilizing the lightweight RV over the altitude range of interest. More than likely, this process will result in minimizing the static margin because the pitch moment of inertia of the lightweight RV cannot be made large enough to satisfy Eqs. (18) and (19) by itself.

Even though the maximum value of the pitch moment of inertia will not satisfy the similarity parameters, the prior static margin constraints lead directly to the maximization of the pitch moment of inertia. By maximizing the pitch moment of inertia, the static margin at the minimum altitude of interest can be increased in length because the influence of the aerodyamic moments on the rotational accelerations is decreased. This increased length at the minimum altitude enables the lightweight RV to remain statically stable over a larger altitude range, i.e., the point of neutral stability occurs below the minimum altitude of interest. The larger altitude range obviously increases the operating range of the lightweight RV, but more importantly, it provides a more robust design that is insensitive to variations in aerodynamic characteristics. To be more specific, the lightweight RV remains statically stable and performs properly even if the aerodynamic and atmospheric models are in error.

In summary, the design rules of thumb are that the moment of inertia ratio of the RVs should be matched, the pitch moment of inertia of the lightweight RV should be maximized, and the static margin of the lightweight RV should be minimized to match the dynamics of the full-weight RV.

IV. Optimization Formulation

The present optimization process is formulated as a typical constrained parameter optimization problem. A performance index of the form

$$J = \int_{t_0}^{t_f} L(\boldsymbol{x}, \boldsymbol{\xi}, t)\,\mathrm{d}t = \int_{t_0}^{t_f} (\boldsymbol{x} - \tilde{\boldsymbol{x}})^T W (\boldsymbol{x} - \tilde{\boldsymbol{x}})\,\mathrm{d}t \qquad (20)$$

is minimized subject to

$$\dot{\boldsymbol{x}} = \boldsymbol{f}_1(\boldsymbol{x}, \boldsymbol{\xi}, t)$$

and

$$\boldsymbol{C}(\boldsymbol{\xi}) \geq \boldsymbol{0}$$

where

$\boldsymbol{C}$ = constraint vector $(b \times 1)$
W = diagonal, positive, semidefinite matrix
$\boldsymbol{x}$ = state vector $(n \times 1)$
$\tilde{\boldsymbol{x}}$ = target state vector $(n \times 1$, known$)$
$\boldsymbol{\xi}$ = parameter vector $(a \times 1$, constants$)$

This performance index is preferable to the norm employed in Eq. (9). The advantage of the L_2 norm for the optimization process is that it provides a smoother (continuous) performance surface than the L_∞ norm and only requires "convergence in the mean."[10] Convergence in the mean enables the designer to judiciously trade off the performance of each velocity history.

The diagonal weight matrix provides the knobs to turn to perform the design tradeoffs. One way to select the values of the diagonal weight matrix is to utilize the weight vector in the SMM formulation. This selection will approximately scale the deviations to one. In this example, the weights applied to the velocity variables were chosen to be one to demonstrate that scaling is not necessary to obtain a converged solution when the similarity parameters are used to initialize the optimization procedure. The diagonal weight matrix used in the optimization process is

$$W = \mathrm{diag}(0, 0, 0, 0, 0, 1, 1, 1, 1, 1, 1)$$

the parameter vector is

$$\boldsymbol{\xi} = (m_1, x_{\mathrm{cm}_1}, I_{xx_1}, I_1)^T$$

and the constraint vector is defined as

$$0 \leq m_1 \leq 0.1 m_2 \qquad x_{\mathrm{cm}_{1\min}} \leq x_{\mathrm{cm}_1} \leq x_{\mathrm{cm}_{1\max}}$$

$$I_{xx_{1_{\min}}} \leq I_{xx_1} \leq I_{xx_{1_{\max}}} \qquad I_{1_{\min}} \leq I_1 \leq I_{1_{\max}}$$

where the minimum and maximum values are determined from the geometric constraints of the vehicle and the available mass. The mass properties and physical dimensions of the full-weight RV are given in Table 1 and Fig. 3, and the constraint values are given in Table 2. Two-sided inequality constraints are used because of the physical constraints of the RV geometry, and in addition, the lower bounds restrict the SQP algorithm to solutions with positive mass properties.

Table 1 Full-weight RV

External dimensions, cm				
r_n	r_b	l_o	l_{cm}	l_d
5	25	91	91	152
Mass properties				
m_2, kg	x_{cm_2}, m	I_{xx_2}, kg · m^2		I_2, kg · m^2
149.96	0.0	2.56		22.477

Table 2 Constraint values

$x_{\mathrm{cm}_{1_{\min}}}$, m	$I_{xx_{1_{\min}}}$, kg · m^2	$I_{1_{\min}}$, kg · m^2
−0.125	0.5	$3.0 + m_1 \lvert x_{\mathrm{cm}_1} \rvert^2_{\max}$
$x_{\mathrm{cm}_{1_{\max}}}$, m	$I_{xx_{1_{\max}}}$, kg · m^2	$I_{1_{\max}}$, kg · m^2
0.125	0.8	$6.0 + m_1 \lvert x_{\mathrm{cm}_1} \rvert^2_{\max}$

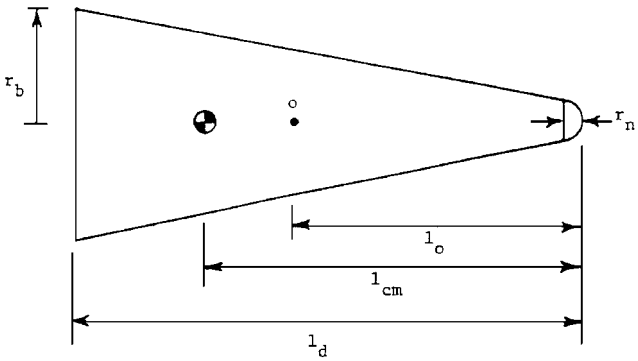

Fig. 3 External dimensions.

V. Results

The results of the optimization process for a 10% weight, axisymmetric RV are given in the following tables and figures. The tracking error is minimized over the altitude range of 400,000–245,000 ft because thrust augmentation is required below 245,000 ft. The shape of the performance surface is presented in Figs. 4–6 for variations in the roll and pitch moments of inertia with the mass and center of mass fixed at 14.97 kg and 0.0 m, respectively. It is readily apparent from Fig. 4 that a well-behaved minimum exists along the constraint boundary, $I = 6.0$ (which corresponds to the design rule of thumb no. 2: maximize the pitch moment of inertia), and the moment of inertia ratio, $I_{xx}/I = 0.1$, defines a valley leading to the minimum, i.e., design rule of thumb no. 1: retain the moment of inertia ratio of the full-weight RV. Figure 5 is a cut along this valley, whereas Fig. 6 is a cut along the constraint plane, $I = 6.0$. As one can see, the region around the minimum is unimodal, smooth, and robust to small variations in the moments of inertia.

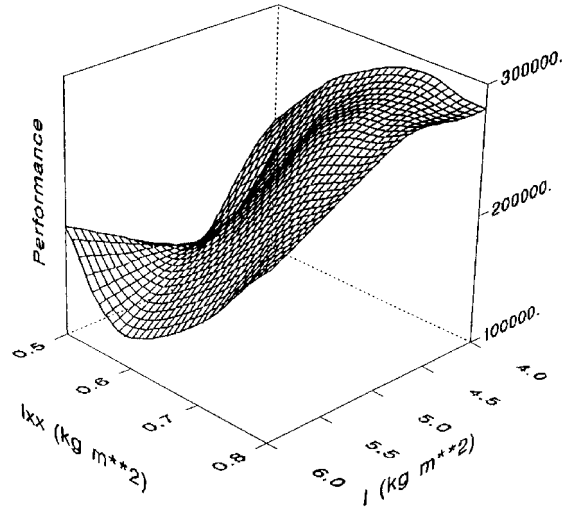

Fig. 4 Performance surface.

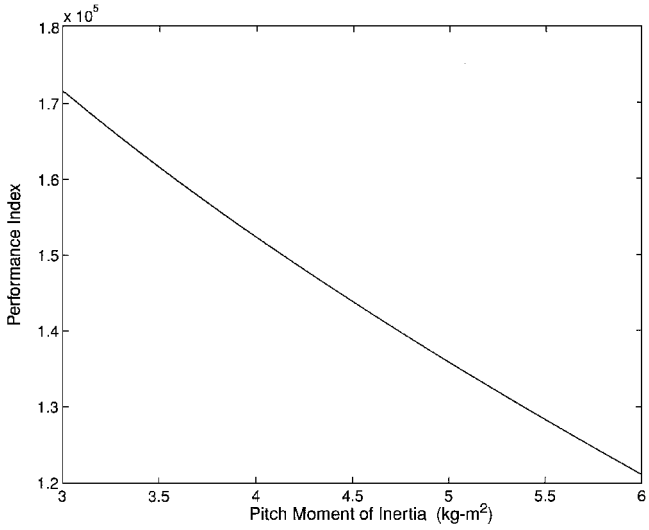

Fig. 5 Constant moment of inertia ratio (0.1).

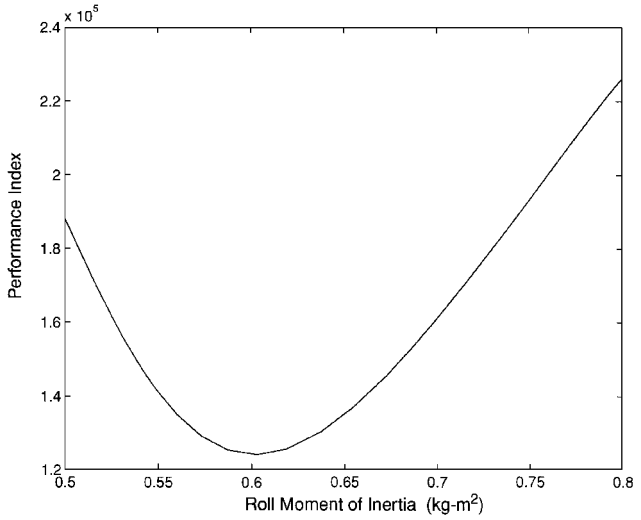

Fig. 6 Constant pitch moment of inertia (6.0).

The mass properties of the full-weight RV and the optimized lightweight RV are given in Table 3 for comparison purposes. A second lightweight RV was developed by perturbing the optimal lightweight RV mass properties. The center of mass was perturbed 20%, which produces approximately 5% variation in the moments of inertia. This RV was simulated to demonstrate the robustness of the design to variations in the mass properties (Table 3). The optimized RV performance is presented in Figs. 7–11. The performances of the

Table 3 Mass properties

Parameter	RV	Optimized LRV	Second LRV
m, kg	149.7	14.97	14.97
x_{cm}, m	0.0	−0.125	−0.100
I_{xx}, kg · m^2	2.560	0.629	0.601
I, kg · m^2	22.500	6.234	6.150
$I_{xx}/(I - mx_{cm}^2)$	0.1138	0.1048	0.1002

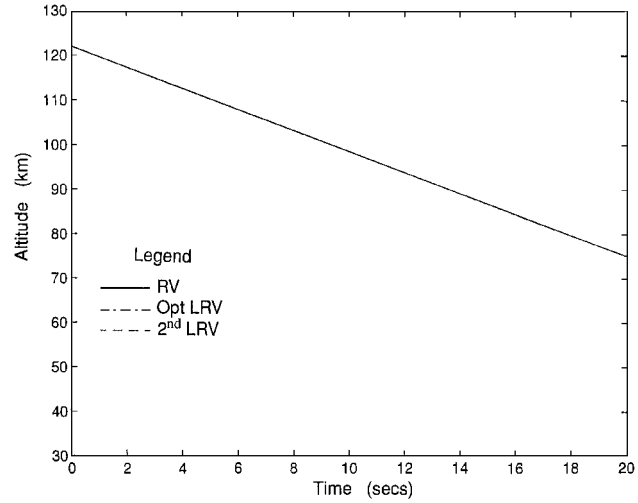

Fig. 7 Altitude time history.

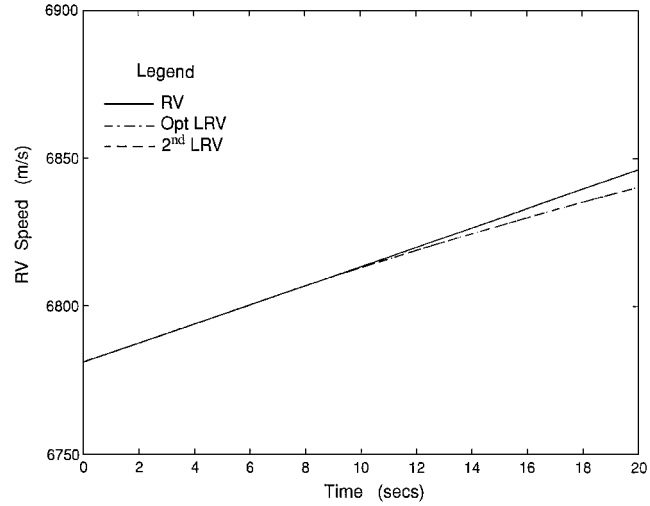

Fig. 8 Speed time history.

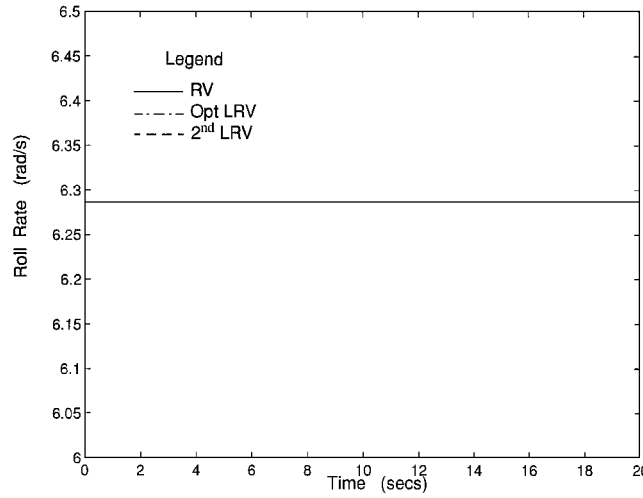

Fig. 9 Body-fixed roll rate time history.

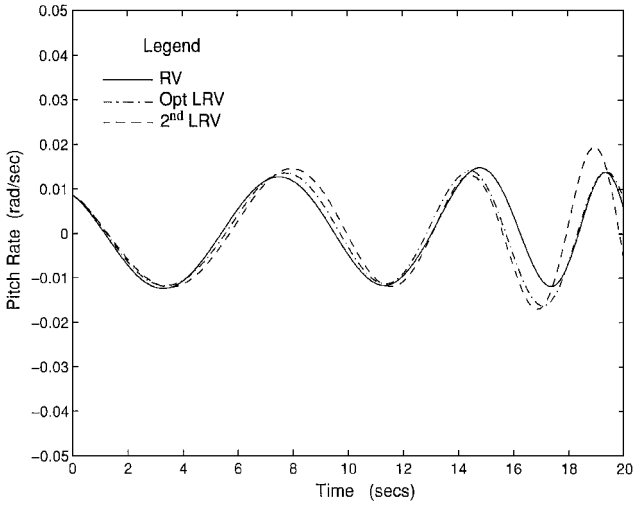

Fig. 10 Pitch rate time history.

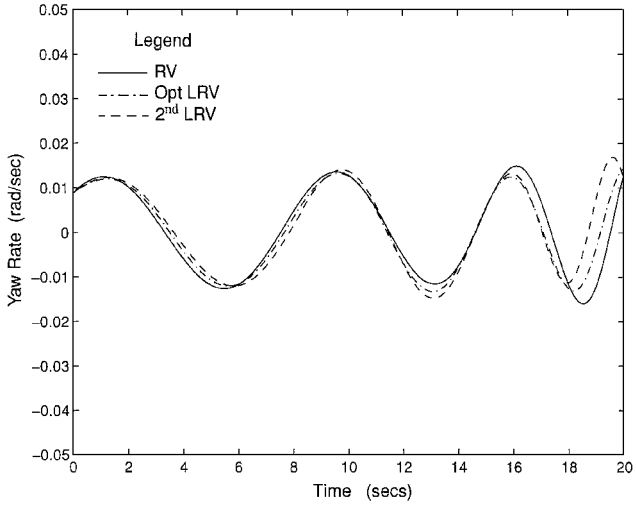

Fig. 11 Yaw rate time history.

two lightweight RVs are nearly equivalent for the first three variables (Figs. 7–9). Note that the lightweight RV speeds drop off because no drag compensation is employed. Figures 10 and 11 show the superior pitch and yaw response matching of this design as compared with the designs of Refs. 5 and 6 because the center of mass position constraint was relaxed to −0.125 m, i.e., design rule of thumb no. 3: minimize the static margin. This center of mass position reduces the static margin of the lightweight RV and better matches the transverse rotational similarity parameters. Also, the robustness of the design is demonstrated by the very good performance of the second lightweight RV with the perturbed parameters.

VI. Conclusions

A new class of six-DOF optimization problems referred to as trajectory matching flight-path optimization was addressed and explicity demonstrated via an example problem. A lightweight RV was designed to match the six-DOF dynamics of a full-weight RV with an optimization procedure that was initialized with similarity parameters. The similarity parameters were developed with a unique stability measure and were used to understand the dominant design parameters and provide excellent initial guesses to the optimization algorithm. The results of this design are superior to the designs of Refs. 5 and 6 because the center of mass location was free to move closer to the center of pressure (reducing the static margin) and, in turn, to reduce the aerodynamic moments (pitch and yaw).

In addition, a set of design rules of thumb was developed during this study. The design rules of thumb are that the mass of the lightweight RV should be maximized, the moment of inertia ratios of the RVs should be matched, the pitch moment of inertia of the lightweight RV should be maximized, and the static margin of the lightweight RV should be minimized to match the dynamics of the full-weight RV. As a result, this study has shown that similarity parameters and six-DOF optimization are effective tools for designing lightweight RVs that are robust to variations in their mass properties.

Acknowledgment

This work was supported by the U.S. Department of Energy under Contract DE-AC0494AL85000.

References

[1]Stengel, R. F., *Stochastic Optimal Control*, Wiley, New York, 1986, pp. 220–238.

[2]Bryson, A. E., Jr., and Ho, Y., *Applied Optimal Control*, Hemisphere, New York, 1975, Chaps. 1–3.

[3]Yeo, B. P., and Sng, K. B., "Numerical Solution of the Constrained Re-Entry Vehicle Trajectory Problem via Quasilinearization," *Journal of Guidance and Control*, Vol. 3, No. 5, 1980, pp. 392–397.

[4]Outka, D. E., "Launch Vehicle Trajectory Optimization," M.S. Thesis, Dept. of Aerospace Engineering and Engineering Mechanics, Univ. of Texas, Austin, TX, Dec. 1984.

[5]Robinett, R. D., "Dynamical Flight Path Optimization of Aerospace Vehicles." AIAA Paper 86-2033, Aug. 1986.

[6]Robinett, R. D., "A Unified Approach to Vehicle Design, Control, and Flight Path Optimization," Ph.D. Dissertation, Dept. of Aerospace Engineering, Texas A&M Univ., College Station, TX, Dec. 1987.

[7]Powell, M. J. D., "A Fast Algorithm for Nonlinearly Constrained Optimization Calculations," *Proceedings of the Biennial Conference on Numerical Analysis*, edited by G. A. Watson, Springer–Verlag, New York, 1978, pp. 144–157.

[8]Regan, F. J., *Re-Entry Vehicle Dynamics*, AIAA Education Series, AIAA, New York, 1984, Chaps. 4 and 7.

[9]Willems, J. L., *Stability Theory of Dynamical Systems*, Wiley, New York, 1970, Chap. 1.

[10]Milne, R. D., *Applied Functional Analysis—An Introductory Treatment*, Pitman, New York, 1980, pp. 115–117.